Appl Biochem Biotechnol (2011) 165:1161–1168
DOI 10.1007/s12010-011-9333-9

Highly Regioselective Synthesis of 3′-*O*-Acyl-Trifluridines Catalyzed by *Pseudomonas cepacia* Lipase

Zhao-Yu Wang · Yan-Hong Bi · Min-Hua Zong

Received: 1 April 2011 / Accepted: 27 July 2011 /
Published online: 6 August 2011

Abstract 3′-*O*-Acyl-trifluridines were prepared successfully through an enzymatic approach for the first time. Among the ten commercially available lipases tested, *Pseudomonas cepacia* lipase displayed the highest regioselectivity towards the acylation of 3′-hydroxyl of trifluridine. Furthermore, the effects of some crucial factors on the enzymatic myristoylation of trifluridine were examined. The optimal reaction medium, molar ratio of trifluridine to vinyl myristate and reaction temperature were found to be anhydrous THF, 1:7 and 50 °C, under which the reaction rate, substrate conversion, and 3′-regioselectivity were 63.9 mM/h, >99.0%, and 99%, respectively. Additionally, the enzyme recognition of the chain length of the acyl donors was investigated. The results showed that 3′-regioselectivity of the enzyme maintained 99% with the increment of acyl chain length (C6, C10, and C14). The reason might derive from the strong hydrophobic interaction between 5-CF_3 group of the base moiety and Leu 287 located in the medium-sized pocket of the active site.

Keywords Trifluridine · Enzymatic regioselective acylation · Substitute · Lipase

Introduction

Trifluridine (TFT), as a kind of pharmacological active analog of deoxynucleoside analogue, is an effective antiviral agent for topical use in the eye [1–4]. Extensively clinical studies have shown that it effectively inhibits DNA replication of herpes simplex virus, which causes primary keratoconjunctivitis and recurrent epithelial keratitis in man [5, 6]. However, like other pharmacological nucleoside drugs, TFT exhibits some disadvan-

Z.-Y. Wang (✉) · Y.-H. Bi
School of Life Science and Chemical Engineering, Huaiyin Institute of Technology, Huai'an 223003, People's Republic China
e-mail: biowzy@126.com

Z.-Y. Wang · M.-H. Zong
Lab of Applied Biocatalysis, South China University of Technology, Guangzhou 510640, People's Republic China

tages in the clinical treatment, such as the difficulty with which it traverses the blood–brain barrier, owing, among others reasons, to its poor lipophilicity, irreversible tissue destruction, and drug-induced cytotoxic side effect [4, 7, 8].

Several strategies to tackle these drawbacks have been carried out to modify nucleoside drugs pharmacological properties [9, 10]. Fortunately, the preparation of its monoesters prodrugs by regioselective acylation with different acyl donors has been proved to be one of the most successful approaches [11]. In particular, it has been proved that the 3′-ester prodrugs of some nucleosides showed more biological activity as compared with the parent agents [12]. On the other hand, the monoprotected nucleosides are the key building blocks for the synthesis of important active chemotherapeutic agents of nucleoside derivatives [13–15].

However, it is usually extremely difficult to selectively acylate 3′-secondary hydroxy group of unprotected TFT directly via the chemical methods, which is characterized by a low regioselectivity, time-consuming protection/deprotection steps, and tedious product isolation [16]. Doubtlessly, enzymatic acylation of unprotected nucleosides in organic media provides a facile and highly efficient methodology owing to the high specificity of enzymes, mild reaction conditions, and environmental friendliness [10, 11, 17]. Gotor and Li have reviewed the use of biocatalysts for the modification of nucleosides [11, 13]. In our ongoing study, we describe the highly regioselective synthesis of 3′-ester of TFT with vinyl myristate by an immobilized lipase from *Pseudomonas cepacia* (PS IM) in organic solvents for the first time. The effects of several crucial factors influencing the enzymatic acylation were also investigated (Scheme 1). Besides, the effect of chain length of the acyl donors (C6, C10 and C14) on the 3′-regioselectivity of the acylation has been examined.

Materials and Methods

Biological and Chemical Materials

An immobilized lipase from *Candida antarctica* (CAL-B), an immobilized lipase from *Thermomyces lanuginosus* (TLL), and an immobilized lipase from *Rhizomucor miehei* (RML) were purchased from Novozymes Co., Ltd., China. PS IM, a powder lipase from *Aspergillus niger*, and a powder lipase from *Mucor javanicus* were purchased from Amamo Enzyme Inc., Japan. A powder lipase from *Candida cylindracea* and a powder lipase from *Porcine pancreas* were obtained from Meito Sangyo Co., Ltd., Japan. A powder lipase from *Penicillium expansum* was kindly donated by Shenzhen Leveking Bioengineering Co., Ltd., China. A powder lipase from *Candida rugosa* was purchased from Sigma (USA). TFT was purchased from Shanghai Hanhong Co., Ltd., China. Vinyl hexanoate, vinyl decanoate, and vinyl myristate were obtained from TCI (Japan). All other chemicals were also from commercial sources and of the highest available purity.

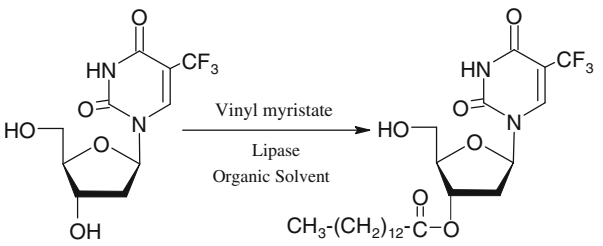

Scheme 1 Enzymatic regioselective acylation of trifluridine with vinyl myristate

General Procedure for Enzymatic Acylation of TFT

In a typical experiment, 2 mL of anhydrous organic solvent (the solvents were dried by gentle shaking with 4 Å molecular sieves overnight.) containing TFT (20 mM), a certain amount of enzyme and vinyl fatty acid ester was incubated in a 10-mL Erlenmeyer shaking flask capped with a septum under predetermined reaction conditions. Aliquots were withdrawn at specified time intervals from the reaction mixture and then diluted by 50 times with corresponding mobile phase prior to HPLC analysis. No chemical acylation was detectable as confirmed by the control experiments.

HPLC Analysis

The reaction mixture was analyzed by RP-HPLC on a 4.6×250-mm (5 μm) Eclips Plus-C18 column (Agilent Technologies Industries Co., Ltd., USA) using an Agilent G1311A pump and a UV Detector at 262 nm. The mobile phase is a mixture of water and methanol at a flow rate of 1.0 ml/min.

The volumetric ratio of water to methanol was 20/80, and the retention times for TFT, 5′-ester, and 3′-ester were 2.33, 3.60, and 3.84 min (hexanoylation), respectively. A gradient elution with water/methanol was used for decanoylation (0–2.0 min, 20/80; 2.0–5.0 min, 0/100) and myristoylation (0–2.0 min, 10/90; 2.0–5.0 min, 0/100). The retention times for TFT, 5′-ester, and 3′-ester were 2.54, 7.18, and 7.42 min (decanoylation); 2.43, 7.19, and 7.58 min (myristoylation), respectively. The regioselectivity was defined as the ratio of the concentration of the desired product to that of all the products. The initial reaction rate (V_0) and the substrate conversion were calculated from the HPLC data.

Purification and Structure Determination of the Esters

The reaction was scaled up by adding 0.4 mmol TFT, 2.8 mmol vinyl fatty acid esters, and 100 U enzyme into 20 mL of anhydrous tetrahydrofuran (THF). On completion of the reaction, the enzyme was filtered off and the filtrate was evaporated under vacuum. The residue was separated and purified by flash column chromatography using ethyl acetate/petroleum ether as the mobile phase. Structural assignments were made on the basis of the changes in the ^{13}C NMR (100 MHz) and ^{1}H NMR (400 MHz) spectra caused by the acylation (Bruker DRX-400 NMR Spectrometer, Bruker Co., Germany).

TFT ^{13}C NMR (DMSO-d_6) δ: 159.13 (C4), 149.75 (C2), 142.33, 142.25 (C6), 124.17, 121.48 (C7), 103.76, 103.30 (C5), 85.71 (C1′), 88.42 (C4′), 70.79 (C3′), 60.67 (C5′), 40.67 (C2′).

3′-O-Hexanoyl-TFT ^{1}H NMR (DMSO-d_6) δ: 11.89 (1H, s, H_3), 8.69 (1H, s, H_6), 6.16 (1H, t, J=6.8 Hz, $H_{1'}$), 5.39 (1H, m, $H_{3'}$), 4.08 (1H, m, $H_{4'}$), 3.67 (2H, m, $H_{5'}$), 2.51 (1H, br s, OH), 2.38–2.31 (2H, m, $H_{2'}$+$H_{2''}$), 1.56–1.53 (2H, m, $H_{3''}$), 1.27–1.24 (4H, br s, $H_{4''}$+$H_{5''}$), 0.85 (3H, t, J=7.0 Hz, $H_{6''}$). ^{13}C NMR (DMSO-d_6) δ: 172.76 ($C_{1''}$), 159.10 (C_4), 149.78 (C_2), 142.28, 142.22 (C_6), 124.14, 121.46 (C_7), 103.66, 103.34 (C_5), 85.74 ($C_{1'}$), 85.61 ($C_{4'}$), 74.71 ($C_{3'}$), 61.21 ($C_{5'}$), 38.14 ($C_{2'}$), 33.57 ($C_{2''}$), 30.82 ($C_{4''}$), 24.19 ($C_{3''}$), 21.97 ($C_{5''}$), 13.86 ($C_{6''}$).

3′-O-Decanoyl-TFT ^{1}H NMR (DMSO-d_6) δ: 11.94 (1H, s, H_3), 8.69 (1H, s, H_6), 6.16 (1H, t, J=6.8 Hz, $H_{1'}$), 5.38 (1H, m, $H_{3'}$), 4.07 (1H, m, $H_{4'}$), 3.66 (2H, m, $H_{5'}$), 2.50 (1H, br s,

OH), 2.38–2.31 (2H, m, $H_{2'}+H_{2''}$), 1.53–1.47 (2H, m, $H_{3''}$), 1.24 (4H, br s, $H_{4''}+H_{5''}$), 0.85 (3H, t, J=6.8 Hz, $H_{6''}$). ^{13}C NMR (DMSO-d_6) δ: 172.53 ($C_{1''}$), 158.93 (C_4), 149.61 (C_2), 142.12, 142.07 (C_6), 124.00, 121.32 (C_7), 103.49, 103.17 (C_5), 85.59 ($C_{1'}$), 85.43 ($C_{4'}$), 74.55 ($C_{3'}$), 61.07 ($C_{5'}$), 38.00 ($C_{2'}$), 33.71 ($C_{2''}$), 31.39 ($C_{8''}$), 29.00–28.67 ($C_{4''}+C_{5''}+C_{6''}+C_{7''}$), 24.58 ($C_{3''}$), 22.19 ($C_{9''}$), 13.93 ($C_{10''}$).

5′-O-Myristoyl-TFT ^{1}H NMR (DMSO-d_6) δ: 11.93 (1H, s, H_3), 8.07 (1H, s, H_6), 6.07 (1H, t, J=6.4 Hz, $H_{1'}$), 5.43 (1H, d, J=4.3 Hz, OH), 4.23–4.22 (3H, m, $H_{3'}+H_{5'}$), 4.05–4.02 (1H, m, $H_{4'}$), 2.30–2.26 (2H, m, $H_{2'}+H_{2''}$), 1.52 (2H, m, $H_{3''}$), 1.25 (20H, br s, $H_{4''}+H_{5''}+H_{6''}+H_{7''}+H_{8''}+H_{9''}+H_{10''}+H_{11''}+H_{12''}+H_{13''}$), 0.86 (3H, apparent t, $H_{14''}$). ^{13}C NMR (DMSO-d_6) δ: 173.90 ($C_{1''}$), 159.12 (C_4), 149.60 (C_2), 141.68, 141.61 (C_6), 131.75, 128.90 (C_7), 102.87, 100.02 (C_5), 86.51 ($C_{1'}$), 84.93 ($C_{4'}$), 69.54 ($C_{3'}$), 62.88 ($C_{5'}$), 39.13 ($C_{2'}$), 33.74 ($C_{2''}$), 31.54 ($C_{12''}$), 29.27–28.59 ($C_{4''}+C_{5''}+C_{6''}+C_{7''}+C_{8''}+C_{9''}+C_{10''}+C_{11''}$), 24.69 ($C_{3''}$), 22.33 ($C_{13''}$), 14.14 ($C_{14''}$).

3′-O-Myristoyl-TFT ^{1}H NMR (DMSO-d_6) δ: 11.91 (1H, s, H_3), 8.68 (1H, s, H_6), 6.16 (1H, t, J=6.8 Hz, $H_{1'}$), 5.39 (1H, m, $H_{3'}$), 4.08 (1H, m, $H_{4'}$), 3.66 (2H, m, $H_{5'}$), 2.50 (1H, br s, OH), 2.39–2.32 (2H, m, $H_{2'}+H_{2''}$), 1.53 (2H, m, $H_{3''}$), 1.24 (4H, br s, $H_{4''}+H_{5''}$), 0.85 (3H, apparent t, $H_{6''}$). ^{13}C NMR (DMSO-d_6) δ: 172.77 ($C_{1''}$), 159.12 (C_4), 149.78 (C_2), 142.33, 142.27 (C_6), 124.18, 121.50 (C_7), 103.63, 103.31 (C_5), 85.73 ($C_{1'}$), 85.63 ($C_{4'}$), 74.68 ($C_{3'}$), 61.21 ($C_{5'}$), 39.07 ($C_{2'}$), 33.64 ($C_{2''}$), 31.54 ($C_{12''}$), 29.26–27.62 ($C_{4''}+C_{5''}+C_{6''}+C_{7''}+C_{8''}+C_{9''}+C_{10''}+C_{11''}$), 24.53 ($C_{3''}$), 22.33 ($C_{13''}$), 14.11 ($C_{14''}$).

Results and Discussion

Regioselectivity of the Acylation of TFT with Various Enzymes

Firstly, several commercially available lipases of different sources were screened for their efficiency in the acylation of TFT with vinyl myristate, including enzyme activity and 3′-regioselectivity (Table 1). The results showed that CAL-B, TLL and PS IM showed good activities as compared with the other enzymes tested. With respect to the position of acylation, the 5′-OH of TFT was preferentially acylated by enzyme of CAL-B (65%), while the favorable formation of 3′-ester was found on PS IM (99%) and TLL (55%).

It was reported that the lipase could functionalize its favorable hydroxyl in the acylation of polyhydroxyl compounds, owing to the specific structure of its active center and the structure of the substrate [18]. Recently, Lavandera et al. uncovered the binding model of the lipase from *P. cepacia* via computer-aided molecular modeling [19]. It was proposed that the special recognizing ability of enzymes could be attributed to favorable substrate orientation in the active centers, due to the difference of the enzyme structures. X-ray crystal structure investigations have revealed that the active site of the PS IM had a large hydrophobic pocket, where the acyl donor binds, a medium-sized pocket in which the base moiety lies and an alternate hydrophobic pocket which can also bind parts of the alcohol moiety [19, 20]. According to the molecular basis of high 3′-regioselectivity of the lipase from *P. cepacia* proposed by Gotor and co-workers, this kind of special structure can effectively reduce the steric strain of the active center to stabilize the 3′-acylation transition state [18, 19]. Since the molecular of the nucleoside is much larger than the medium-sized

Table 1 Regioselective myristoylation of TFT catalyzed by various lipases

Enzyme	V_0 (mM/h)	Conv.[a] (%)	Regioselectivity (%)	
			5′-	3′-
CAL-B	39.3	55.2	65	34
RML	11.8	24.3	57	43
PS IM	43.4	68.0	n.d.	99
TLL	58.1	73.3	45	55
Lipase MY	4.3	13.9	23	77
Lipase A	n.d.	n.d.	n.d.	n.d.
Lipase M	n.d.	n.d.	n.d.	n.d.
Lipase LVK	n.d.	n.d.	n.d.	n.d.
CRL-VII	n.d.	n.d.	n.d.	n.d.
PPL	n.d.	n.d.	n.d.	n.d.

The reactions were carried out at 40 °C and 200 rpm by adding 0.04 mmol TFT, 0.12 mmol vinyl myristate, and 50 U enzyme into 2 ml of anhydrous THF

CAL-B immobilized lipase from *Candida antarctica*, *RML* immobilized lipase from *Rhizomucor miehei*, *PS IM* immobilized lipase from *P. cepacia*, *TLL* immobilized lipase from *Thermomyces lanuginosus*, *Lipase MY* powder lipase from *Candida cylindracea*, *Lipase A* powder lipase from *Aspergillus niger*, *Lipase M* powder lipase from *Mucor javanicus*, *Lipase LVK* powder, lipase from *Penicillium expansum*, *CRL-VII* powder, lipase from *Candida rugosa*, *PPL* powder lipase from *Porcine pancreas*, *n.d.* not detected

[a] Maximum substrate conversion

pocket, the base moiety extend into alternate hydrophobic pocket (in which the catalytic residue Leu 287 lies) in 3′-acylation transition state. Thus, the strong hydrophobic interaction between CF_3 group of the base moiety and the hydrophobic side chain of Leu 287 located in the alternate hydrophobic pocket of the active site as well as the destabilization of the conformation of 5′-acylation transition state resulted from the mutual action between the base moiety and a longer acyl group would stabilize the 3′-acylation transition state and thus increasing the 3′-regioselectivity.

Effect of Reaction Medium

It is well known that the properties of solvents have significant effects on the catalytic characteristics of enzymes [21, 22]. One of the most impracticable limitations in the acylation of hydrophilic nucleosides is their poor solubility in hydrophobic solvent, which is advantageous to the stabilization of enzyme. Eight solvents with log *P* ranging from −1.30 to 0.71 were selected to investigate the influence on the activity and 3′-regioselectivity of the PS IM.

As evident from the data listed in Table 2, the initial rate, maximum substrate conversion, and the 3′-regioselectivity of the acylation were not correlated with log *P* of the solvents, a commonly used solvent parameter in the field of non-aqueous enzymology. No ester derivatives were obtained in DMSO, DMF, and pyridine due to the inactivation of the biocatalyst as confirmed experimentally. Among the other media examined, the absolute 3′-regioselectivity (99%) and good conversion (68.0%) were achieved with enzymatic acylation of TFT in THF. Although higher 3′-regioselectivity (95%) was observed with *tert*-butanol being the reaction medium, its viscosity causing severe mass transfer limitation resulted in low reaction rate and conversion of the acylation [23].

Table 2 Effect of organic solvents on PS IM-catalyzed regioselective acylation of TFT with vinyl myristoylation

Solvent	Log *P*	V_0 (mM/h)	Conv. (%)	3′-Regioselectivity (%)
DMSO	−1.30	n.d.	n.d.	n.d.
Dioxane	−1.10	29.7	54.0	93
DMF	−1.00	n.d.	n.d.	n.d.
Acetonitrile	−0.33	50.5	69.7	90
Acetone	−0.23	49.9	72.0	92
THF	0.49	43.4	68.0	99
tert-Butanol	0.60	22.8	43.4	95
Pyridine	0.71	n.d.	n.d.	n.d.

The reactions were carried out at 40 °C, 200 rpm by adding 0.04 mmol TFT, 0.12 mmol vinyl myristate, and 50 U PS IM into 2 ml of anhydrous solvents

DMF dimethyleformamide, *THF* tetrahydrofuran

Effect of the Molar Ratio of Vinyl Myristate to TFT

Parallel to enzymatic acylation of nucleosides with vinyl esters, there exists a side reaction, i.e., the hydrolysis of acyl donors catalysed by the enzyme [24]. Hence, an excessive amount of acyl donors is normally necessary for enzymatic acylation of nucleosides. As shown in Fig. 1, remarkable enhancement in both the initial rate and the substrate conversion was observed with the increasing ratio up to 7, the optimal ratio of vinyl myristate to TFT. Additionally, the molar ratio of vinyl myristate to TFT had little effect on the 3′-regioselectivity (99%) of the reaction.

Effect of Reaction Temperature

Reaction temperature has a significant influence on the activity, selectivity and stability of an enzyme and the reaction equilibrium as well. As can be seen in Fig. 2, the initial reaction rate increased rapidly with increasing reaction temperature up to 50 °C, beyond which a further

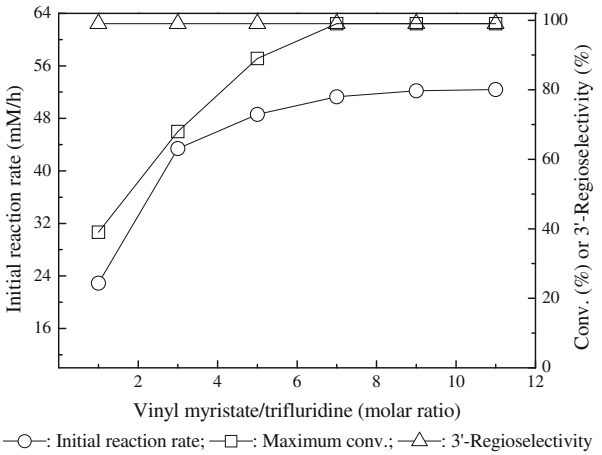

Fig. 1 Effect of the molar ratio of vinyl myristate to TFT on PS IM-catalyzed acylation of TFT. The reactions were carried out at 40 °C, 200 rpm by adding 0.04 mmol TFT, 50 U PS IM, various amount of vinyl myristate into 2 ml of anhydrous THF

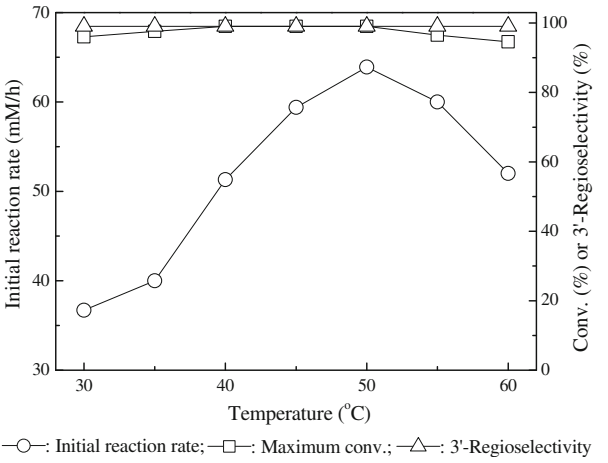

Fig. 2 Effect of the temperatures on PS IM-catalyzed acylation of TFT with vinyl myristate. The reactions were carried out at 200 rpm, various temperatures from 30 to 60 °C by adding 50 U PS IM, 0.04 mmol TFT, and 0.28 mmol vinyl myristate into 2 ml of anhydrous THF

rise in reaction temperature led to a sharp drop in initial reaction rate, suggesting the partial deactivation of the lipase in organic solvents at high temperatures. Interestingly, within the assayed range the reaction temperature showed no effect on the 3′-regioselectivity (99%).

Effect of Chain Length of the Acyl Donor

In order to verify the relationship between the acyl donors and the 3′-regioselectivity, various aliphatic chains of the acyl donors were examined in the regioselective acylation of TFT.

As shown in Table 3, TFT could be converted to the desired product in excellent conversion (>99.0%) in the reaction catalyzed by PS IM. Furthermore, the initial reaction rate dropped with the elongation of chain length of vinyl esters from C6 to C14, perhaps because a longer acyl donor, such as vinyl myristate, is more difficult to enter into the active site to form the first tetrahedral intermediate (generally considered as the rate-limiting step), due to the steric hindrance [23, 25]. Surprisingly, the 3′-regioselectivity on the acylation of TFT exclusively maintained 99% with all the used acyl donors. Li et al. has reported that the 3′-regioselectivity increased with the lengthening chain of the acyl donors (from C2 to C18) in the formation of 3′-*O*-esters of the FUdR [26]. The unexpected results indicated that the substituent (CF_3 vs. F) of the nucleoside in five-position played a crucial role in the reaction catalyzed by lipase from *P. cepacia*, and 3′-regioselectivity of PS IM was enhanced with the increase of the hydrophobicity of CF_3 (CF_3>F). According to the substrate-binding model proposed by Lavandera et al. [18, 19], the more hydrophobic 5-substituent, the stronger its interactions with Leu 287 in the enzyme active site, which stabilizes the acyl-enzyme intermediate better and thus resulted in higher 3′-regioselectivity.

Table 3 Effect of various chian lengths of acyl donors on PS IM-catalyzed regioselective acylation of TFT

Entry	Acyl donor	V_0 (mM/h)	Conv. (%)	3′-Regioselectivity (%)
1	Vinyl hexanoate (C6)	79.1	>99.0	99
2	Vinyl decanoate (C10)	70.2	>99.0	99
3	Vinyl myristate (C14)	63.9	>99.0	99

The reactions were carried out at 50 °C and 200 rpm by adding 0.04 mmol TFT, 0.28 mmol acyl donor, and 50 U PS IM into 2 ml of anhydrous THF

Conclusions

In the process of PS IM-catalyzed transesterification for 3′-*O*-ester prodrugs preparation of the TFT, enzymatic route has been proved to be facile and efficient as compared with the multi-step chemical procedure. The five-substitute group of the base moiety of the CF_3 exerts a significant impact on the 3′-regioselectivity of the acylation. These findings may help to control the catalytic regioselectivity of the synthetically useful enzyme by substrate engineering and protein engineering approaches.

Acknowledgments We thank the Natural Science Research Project of Higher Education of Jiangsu (grant no. 10KJB530001), National Natural Science Foundation of China (grant nos. 20676043 and 20876059), and Science and Technology Project of Guangzhou city (grant no. 2007Z3-E4101) for financial support.

References

1. Anand, B. S., Katragadda, S., Gunda, S., & Mitra, A. K. (2006). *Molecular Pharmaceutics, 3*, 431–440.
2. Altmann, S., Brandt, C. R., Murphy, C. J., Patnaikuni, R., Takla, T., Toomey, M., et al. (2011). *Journal of Infectious Diseases, 203*, 683–690.
3. De Clercq, E. (2011). *Annual Review of Pharmacology and Toxicology, 51*, 1–24.
4. Carmine, A. A., Brogden, R. N., Heel, R. C., Speight, T. M., & Avery, G. S. (1982). *Drugs, 23*, 329–353.
5. Hobden, J. A., Kumar, M., Kaufman, H. E., Clement, C., Varnell, E. D., Bhattacharjee, P. S., et al. (2011). *Investigative Ophthalmology & Visual Science, 52*, 830–833.
6. Skevaki, C. L., Galani, I. E., Pararas, M. V., Giannopoulou, K. P., & Tsakris, A. (2011). *Drugs, 71*, 331–347.
7. Sangwan, V. S., & Basu, S. (2011). *British Journal of Ophthalmology, 95*, 1–2.
8. Mencucci, R., Paladini, I., Menchini, U., Gicquel, J. J., & Dei, R. (2011). *British Journal of Ophthalmology, 95*, 28–31.
9. Kumar, V., Parmar, V. S., & Malhotra, S. V. (2010). *Biochimie, 92*, 1260–1265.
10. Gotor, V. (2002). *Organic Process Research and Development, 6*, 420–426.
11. Li, N., Smith, T. J., & Zong, M. H. (2010). *Biotechnology Advances, 28*, 348–366.
12. Hamamura, E. K., Prystasz, M., Verheyden, J. P. H., Moffatt, J. G., Yamaguchi, K., Uchida, N., et al. (1976). *Journal of Medicinal Chemistry, 19*, 654–662.
13. Ferrero, M., & Gotor, V. (2000). *Monatshefte Für Chemie, 131*, 585–616.
14. Díaz-Rodríguez, A., Fernández, S., Sanghvi, Y. S., Ferrero, M., & Gotor, V. (2006). *Organic Process Research and Development, 10*, 581–587.
15. Quan, J., Wang, N., Cai, X. Q., Wu, Q., & Lin, X. F. (2007). *Journal of Molecular Catalysis B: Enzymatic, 44*, 1–7.
16. Ozaki, S., Akiyama, T., Morita, T., Kumegawa, M., Nagase, T., Uehara, N., et al. (1990). *Chemical & Pharmaceutical Bulletin, 38*, 3164–3166.
17. Ferrero, M., & Gotor, V. (2000). *Chemical Reviews, 100*, 4319–4348.
18. Lavandera, I., Fernandez, S., Magdalena, J., Ferrero, M., Kazlauskas, R. J., & Gotor, V. (2005). *ChemBioChem, 6*, 1381–1390.
19. Lavandera, I., Fernandez, S., Magdalena, J., Ferrero, M., Grewal, H., Savile, C. K., et al. (2006). *ChemBioChem, 7*, 693–698.
20. Kim, K. K., Song, H. K., Shin, D. H., Hwang, K. Y., & Suh, S. W. (1997). *Structure, 5*, 173–185.
21. Klibanov, A. M. (1997). *Trends in Biotechnology, 15*, 97–101.
22. Klibanov, A. M. (2001). *Nature, 409*, 241–246.
23. Wang, Z. Y., Li, N., & Zong, M. H. (2009). *Journal of Molecular Catalysis B: Enzymatic, 59*, 212–219.
24. Weber, H. K., Weber, H., & Kazlauskas, R. J. (1999). *Tetrahedron-Asymmetry, 10*, 2635–2638.
25. Wang, Z. Y., & Zong, M. H. (2009). *Biotechnology Progress, 25*, 784–791.
26. Li, N., Zong, M. H., & Ma, D. (2009). *Tetrahedron, 65*, 1063–1068.